Channels 8:5, 414–420; September/October 2014; Published with license by Taylor & Francis Group, LLC

Functional interaction between S1 and S4 segments in voltage-gated sodium channels revealed by human channelopathies

Mohamed-Yassine Amarouch[1,#], Marina A Kasimova[2,3], Mounir Tarek[2,4], and Hugues Abriel[1,*]

[1]Department of Clinical Research; University of Bern; Bern, Switzerland; [2]Université de Lorraine; Structure et Réactivitè des Systèmes Moléculaires Complexes (SRSMC); Unité Mixte de Recherche (UMR) 7565; Vandoeuvre-lès-Nancy, France; [3]Department of Biology; Lomonosov Moscow State University; Moscow, Russia; [4]Centre National de Recherche Scientifique (CNRS); Structure et Réactivité des Systèmes Moléculaires Complexes (SRSMC); Unité Mixte de Recherche (UMR) 7565; Vandoeuvre-lès-Nancy, France;

[#]Current address: Equipe de Recherche, Substances Naturelles & Environnement; Université Sidi Mohamed Ben Abdellah de Fès; Faculté Polydisciplinaire de Taza; Taza, Morocco

Keywords: cellular electrophysiology, channelopathies, molecular dynamics, S1-S2 segments, sodium channels, voltage-sensing domain

The p.I141V mutation of the voltage-gated sodium channel is associated with several clinical hyper-excitability phenotypes. To understand the structural bases of the p.I141V biophysical alterations, molecular dynamics simulations were performed. These simulations predicted that the p.I141V substitution induces the formation of a hydrogen bond between the Y168 residue of the S2 segment and the R225 residue of the S4 segment. We generated a p.I141V-Y168F double mutant for both the $Na_v1.4$ and $Na_v1.5$ channels. The double mutants demonstrated the abolition of the functional effects of the p.I141V mutation, consistent with the formation of a specific interaction between Y168-S2 and R225-S4. The single p.Y168F mutation, however, positively shifted the activation curve, suggesting a compensatory role of these residues on the stability of the voltage-sensing domain.

Introduction

In excitable tissues, the upstroke of the action potential is the result of the passage of a large and rapid influx of sodium ions (I_{Na}) through voltage-gated sodium channels (Na_V). Na_V dysfunction has been associated with an increasingly wide range of neurological, muscular and cardiac disorders. Mutations in the genes SCN1A, SCN4A and SCN5A, which encode $Na_V1.1$, $Na_V1.4$ and $Na_V1.5$, respectively, lead to various epilepsy syndromes, muscular disorders and inherited cardiac arrhythmias.[1-3]

Na_V channels are monomers with a tetrameric repeat of 6 transmembrane (TM) segments. The first 4 TM segments (S1-S4) comprise the voltage-sensing domain (VSD), and the last 2 TM segments (S5 and S6) form the pore of the channel when assembled in a tetrameric configuration. The S1 segment of domain I contains amino acids that are highly conserved between different species and different Na_V isoforms. One of these amino acids is isoleucine 141. Its substitution to valine in $Na_V1.4$, $Na_V1.5$ and $Na_V1.7$ channels has been linked to inherited channelopathies in patients with hyper-excitability phenotypes, i.e. myotonia, exercise-induced polymorphic ventricular arrhythmias and erythromelalgia.[1-6]

The p.I141V mutation in $Na_V1.4$ and $Na_V1.5$, as well as its homologous p.I136V mutation in $Na_v1.7$, induce similar modifications in the biophysical properties of the voltage-gated sodium channels[3-6] by shifting the voltage-dependence of steady state activation toward more negative potentials and hastening the activation and inactivation kinetics. In addition, the I_{Na} generated by these mutant channels have larger sodium window current peaks which are shifted toward more negative potentials. These observations highlight the important role of isoleucine 141 in the gating process of Na_v channels.

The recently published crystal structure of the bacterial Na_vAb channel demonstrates close proximity between the S1 and S4 segments of the VSD.[7] Based on the fact that Na_vAb can be used as a homolog for the mammalian $Na_V1.4$, $Na_V1.5$ and $Na_V1.7$ channels, we generated a model of $Na_v1.4$ and investigated the interplay between the p.I141V mutation and the stability of its VSDs. Through molecular dynamics (MD) modeling and biophysical characterization, we strived to determine if a modification of intra-segment interactions inside the VSD domain could stabilize

*Correspondence to: Hugues Abriel; Email: Hugues.Abriel@dkf.unibe.ch
Submitted: 07/23/2014; Revised: 08/22/2014; Accepted: 08/22/2014
http://dx.doi.org/10.4161/19336950.2014.958922

the activated state of the channel that carries the p.I141V mutation.

Results

The p.I141V mutation stabilizes the activated state of $Na_v1.4$ and $Na_v1.5$

The functional effects of the p.I141V mutation on $Na_v1.4$ and $Na_v1.5$ were investigated using the whole-cell configuration of the patch-clamp technique. The initial step was to reproduce, under similar experimental conditions, previously published data regarding the effect of the p.I141V mutation on the voltage dependence of activation and inactivation of $Na_v1.4$ and $Na_v1.5$ found in patients with myotonia and cardiac arrhythmias (**Fig. 1A-F**).[3,4] For both channels, the presence of the p.I141V mutation shifted the voltage dependence of activation toward negative potentials ($Na_v1.4$-$V_{1/2\ act}$: -18 ± 1.4 mV, n = 9, versus -28 ± 2.1 mV, n = 5, $^{***}P < 0.001$; slope: 5.3 ±

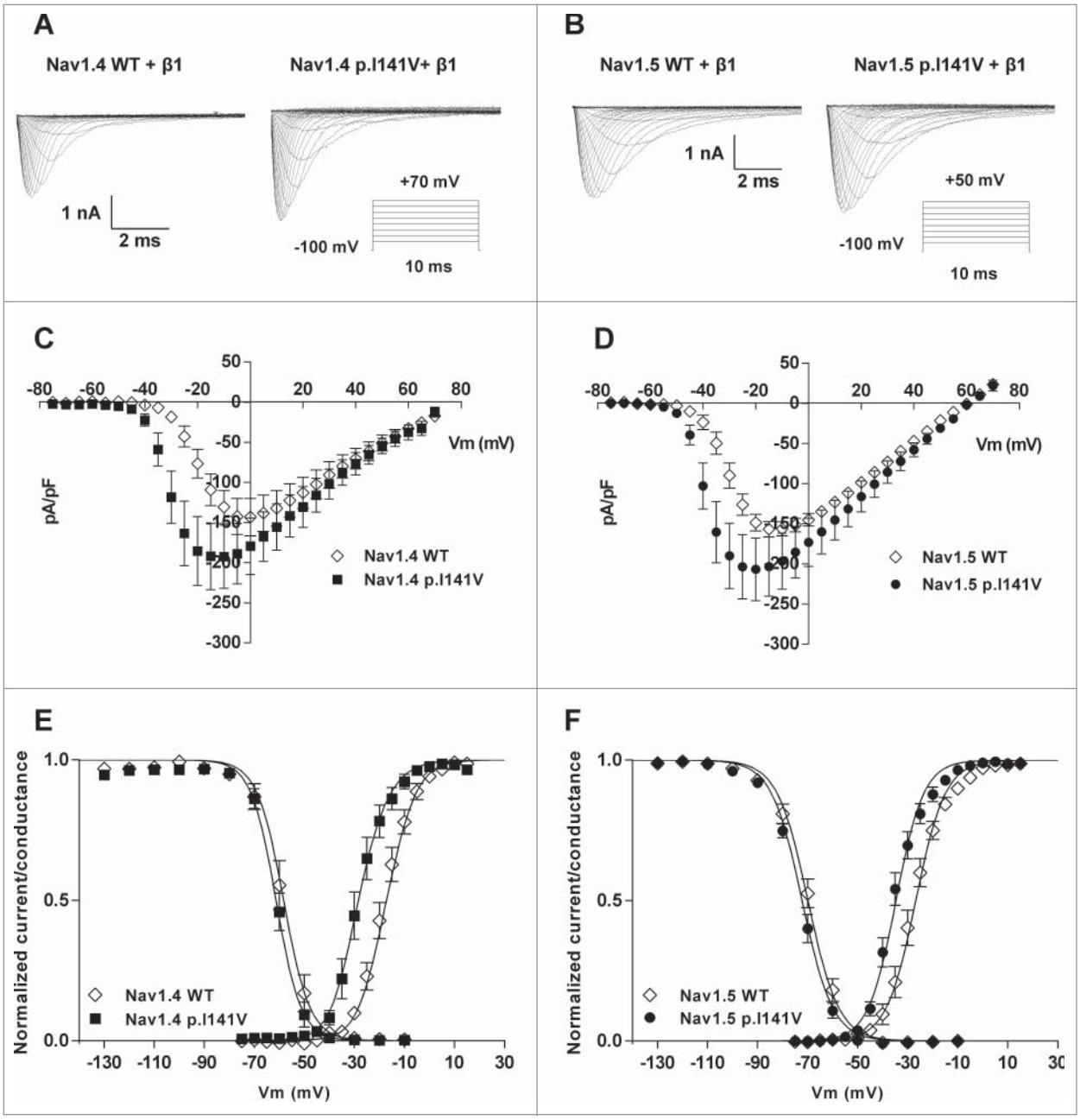

Figure 1. (**A and B**) Representative current traces obtained with protocol in inset using HEK293 cells transfected with $Na_v1.4$-WT and $Na_v1.4$-I141V (**A**); $Na_v1.5$-WT and $Na_v1.5$-I141V (**B**). (**C and D**) Current-voltage (I/V) relationships curves of $Na_v1.4$-WT and $Na_v1.4$-I141V (**C**); $Na_v1.5$-WT and $Na_v1.5$-I141V (**D**). (**E and F**) Steady-state activation and inactivation curves for $Na_v1.4$ (**E**) and $Na_v1.5$ (**F**). Activation properties were determined from I/V relationships by normalizing peak I_{Na} to driving force and maximal I_{Na}. The protocol for the voltage-dependence of steady state of inactivation was 20-ms test pulse to 0 mV ($Na_v1.4$) or −10 mV ($Na_v1.5$) after a 500 ms conditioning pre-pulse.

0.4 mV vs. 5.4 ± 0.5 mV, for WT and mutant channels, respectively, **Fig. 1E**; $Na_v1.5$-$V_{1/2\ act}$: −27 ± 1.3 mV, n = 10, versus −35 ± 1.3 mV, n = 9, $^{***}P < 0.001$; slope: 5.9 ± 0.1 mV vs. 5.5 ± 0.3 mV, for WT and mutant channels, respectively, **Fig. 1F**). The voltage dependence of steady-state inactivation in the presence of the p.I141V mutation was not modified ($Na_v1.4$-$V_{1/2\ inact}$: −59 ± 1.9 mV, n = 7, versus −60 ± 1 mV, n = 4; slope: 5 ± 0.2 mV vs. 4.8 ± 0.2 mV, for WT and mutant channels, respectively, **Fig. 1E**; $Na_v1.5$-$V_{1/2\ inact}$: −70 ± 1.4 mV, n = 9, versus −72 ± 0.9 mV, n = 9, slope: 6.3 ± 0.4 mV vs. 6.1 ± 0.5 mV, for WT and mutant channels, respectively, **Fig. 1F**).

Effect of the p.I141V mutation as predicted by molecular dynamics simulations

To investigate the structural and functional effects of the p.I141V mutation on voltage gated sodium channels, an atomistic model of the $Na_v1.4$ channel was built (see Methods section). The final selected structure of $Na_v1.4$ was based on the scoring functions and the analysis of the Ramachandran plots. This structure corresponded to the activated/closed state of the channel and served as the Na_vAb template for the homology modeling method. The isoleucine 141 residue of $Na_v1.4$ was mutated into valine and MD calculations were performed for the 2 forms of the channel: the WT and the p.I141V mutant. Both structures were embedded in a model membrane formed by a palmitoyl-oleyl-phosphatidylcholine (POPC) bilayer and surrounded by a 150 mM KCl (symmetric) solution (**Fig. 2A**).

In both the Na_vAb crystal structure and $Na_v1.4$ models, I141 was in close proximity to the Y168 and R225 residues, which are crucial for the VSD function (**Fig. 2B** and **C**). R225 is one of the S4 positive residues that participate in the charge transfer, and Y168 corresponds to F233 in the Kv1.2/Kv2.1 paddle chimera that serves as a hydrophobic plug, across which R255 residue must transit.[8] Alteration of the interaction between these residues might influence activation and deactivation of the VSD. For this reason, the evolution of non-bonded interaction energy between Y168 and R225 during the MD runs of the WT and p.I141V mutant were monitored. The Y168 – R225 interaction energy of the WT structure was ∼0 kcal/mol, suggesting no specific interaction; whereas that of the mutant sharply dropped to ∼ −4.5 kcal/mol within the first ns of the MD run (**Fig. 2D**). The drop in energy is consistent with the formation of a hydrogen bond. The distance between the hydrogen atom of the Y168 hydroxyl group and the oxygen atom of the R225 backbone (**Fig. 2E**) also supports this model.

The MD simulations suggest that the mutagenesis of isoleucine 141 to valine, a less bulky residue, modifies the equilibrium position of Y168 with respect to R225. With the p.I141V mutant, these residues come close enough to initiate the formation of a hydrogen bond between their groups; whereas with the WT channel, the formation of such an interaction is sterically hindered by the bulkier isoleucine residue.

The p.Y168F mutation destabilizes the VSD and abolishes the functional effect of the p.I141V mutation in $Na_v1.4$ and $Na_v1.5$

The MD simulations suggest that the p.I141V activated state is more stable than the WT. The stabilization of the DI VSD is proposed to be caused by the formation of a hydrogen bond between Y168 of the S2 segment (S2-DI) and R225 of the S4 segment (S4-DI) (**Fig. 2C**). To test this hypothesis, the $Na_v1.4$ and $Na_v1.5$ channels were mutated by substituting the Y168 residues for phenylalanines. The double mutant p.I141V-Y168F was also generated in order to prevent formation of the hypothetical hydrogen bond between Y168 and R225. Interestingly, the biophysical characterization of the p.I141V-Y168F double mutants showed abolition of the p.I141V effect on the $Na_v1.4$ and $Na_v1.5$ channels (**Fig. 3A-F**). The calculated half-potential values of the steady state of activation and inactivation of the WT channels and the p.I141V-Y168F mutants were not statistically different. The slope of the activation curve for $Na_v1.4$ was not significantly modified. The voltage dependence of activation was shifted toward more positive potentials for the single mutant p.Y168F (**Table 1**, **Fig. 3C-F**), but the voltage dependencies of inactivation were not affected for the mutants nor the WT (**Table 1**, **Fig. 3E** and **F**).

Discussion

The substitution of the highly conserved isoleucine 141 to valine in the $Na_v1.4$, $Na_v1.5$ and Nav1.7 channels has been associated with several inherited disorders of excitability, such as myotonia, cardiac arrhythmias, and erythromelalgia.[3–6] This study investigated the biophysical effects of the p.I141V mutant on these channels and demonstrated that the p.I141V substitution stabilized the activated state of the DI VSD, manifested by a negative shift of the voltage dependence of the activation curve.

The crystal structure of the bacterial channel Na_vAb, published by the Catterall group, shows close proximity between segments S1 and S4 of the VSD.[7] Based on this observation, the hypothesis that the p.I141V substitution stabilizes the open conformation of the mammalian voltage-gated sodium channel $Na_v1.4$ by modifying or creating new interactions between these specific segments was tested. An atomistic model of $Na_v1.4$ was built using homology modeling and the structure of the Na_vAb channel as a template. Unconstrained atomistic MD simulation data suggested that the p.I141V mutation influences the position of the Y168 residue in S2-DI. The Y168 residue was predicted to be spatially closer to R225 of the S4 segment in the mutant VSD, allowing for the formation of a hydrogen bond between the Y168 hydroxyl group and the R225 backbone. The observed hydrogen bond could be responsible for the stabilization of the activated state of the mutant channel in comparison to the WT. Therefore, to abolish the effect of the p.I141V mutation, the formation of a hydrogen bond in the mutant should be prevented.

Based on these predictions, a single (p.Y168F) and double mutant (p.I141V-Y168F) were generated in order to suppress

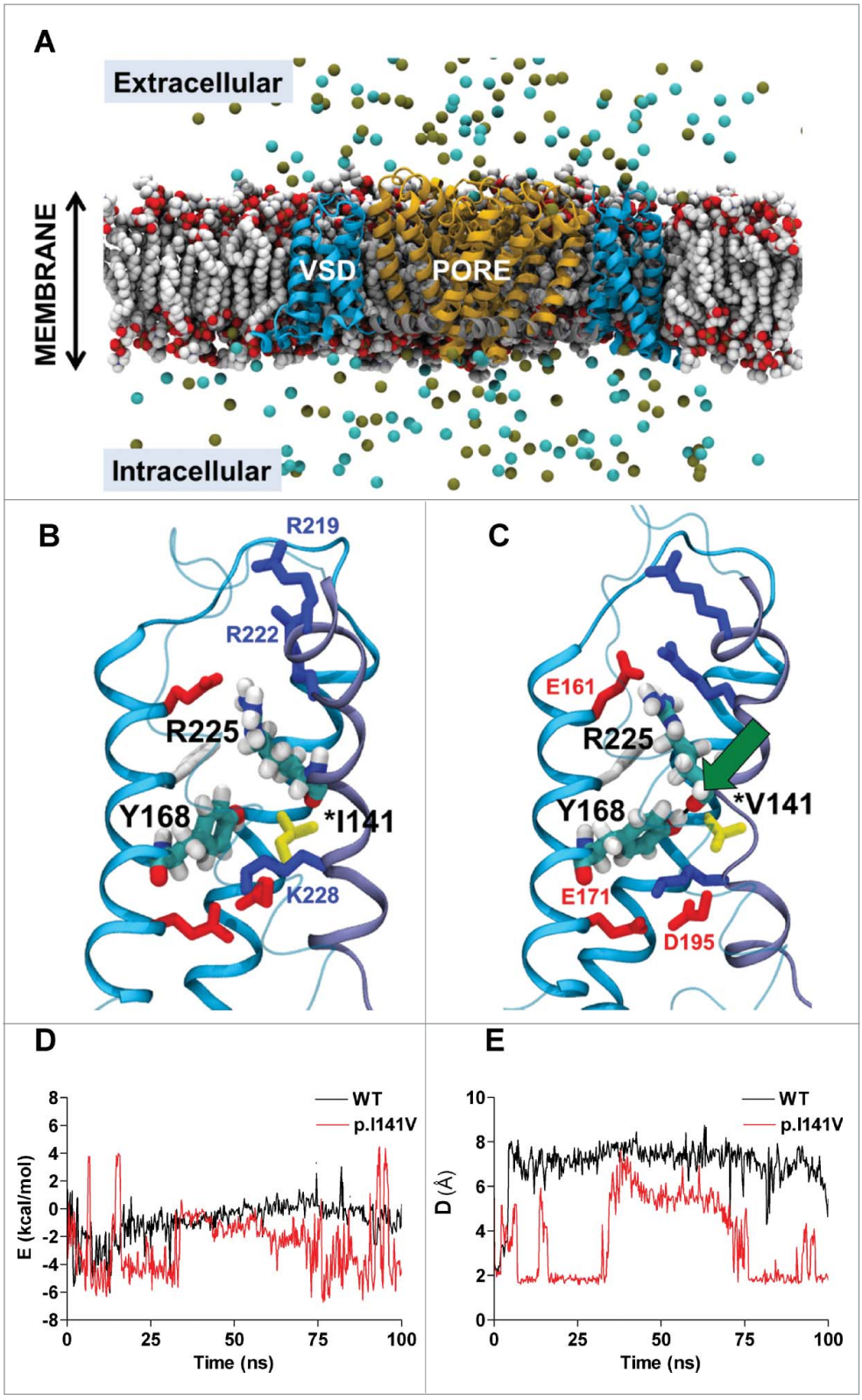

Figure 2. (**A**) $Na_v1.4$ configuration embedded in a POPC lipid bilayer (white; ball representation), surrounded with a 150 mM KCl solution (K^+ tan and Cl^- cyan; water not shown). The pore domain (yellow), S4-S5 (gray) and the VSD (light blue) are drawn as ribbon. (**B and C**), VSD configurations of the WT (**B**) and the p.I141V mutant (**C**), highlighting the S4 residues R219, R222, R225 and K228, and their negatively charged counterparts E161, E171, and D195 of S2 and S3. In the WT, I141 (yellow) prevents Y168 from interacting with R225 (both residues are all in atom stick representation for clarity). In the I141V mutant, the hydrogen atom of the Y168 hydroxyl group and the oxygen atom of R225 backbone are ~2.0 Å apart. This allows for the formation of a hydrogen bond (the green arrow) that stabilizes the confirmation. (**D**) Non-bonded interaction energy between Y168 and R225 from the MD simulations of the WT (black) and the I141V mutant (red). Notably, the energy reaches −4.5 kcal/mol when the pair distance is short. (**E**) Distance between the hydrogen atom of the Y168 hydroxyl group and the oxygen atom of the R225 backbone from the MD simulations of the WT (black) and the I141V mutant (red). Notably, the distance drops intermittently to ~2 Å for the mutant, indicating the formation of a hydrogen bond.

the hydroxyl group of tyrosine, which was found to form a hydrogen bond with R225. The functional analyses of these mutant channels demonstrated the abolition of the p.I141V effect on the voltage dependency of activation for both the $Na_v1.4$ and $Na_v1.5$ channels. The recovery of the WT biophysical parameters in the double mutant (p.I141V-Y168F) is consistent with the MD simulation predictions.

The functional experimental data of the single mutation (p.Y168F) showed a destabilization of the activated state of the $Na_v1.4$ and $Na_v1.5$ channels. This was reflected by a significant shift of the activation curves to more depolarized potentials. This effect was unexpected and raises the question of whether the neutralization of the biophysical effect of the p.I141V mutant is due to the abolition of a newly formed hydrogen bond or due to an additive effect of the p.I141V and p.Y168F mutants on sodium channel function. Given that the double mutation p.I141V-Y168F significantly modified the slope of the activation curve of $Na_v1.4$, the hypothesis that the recovery of WT behavior

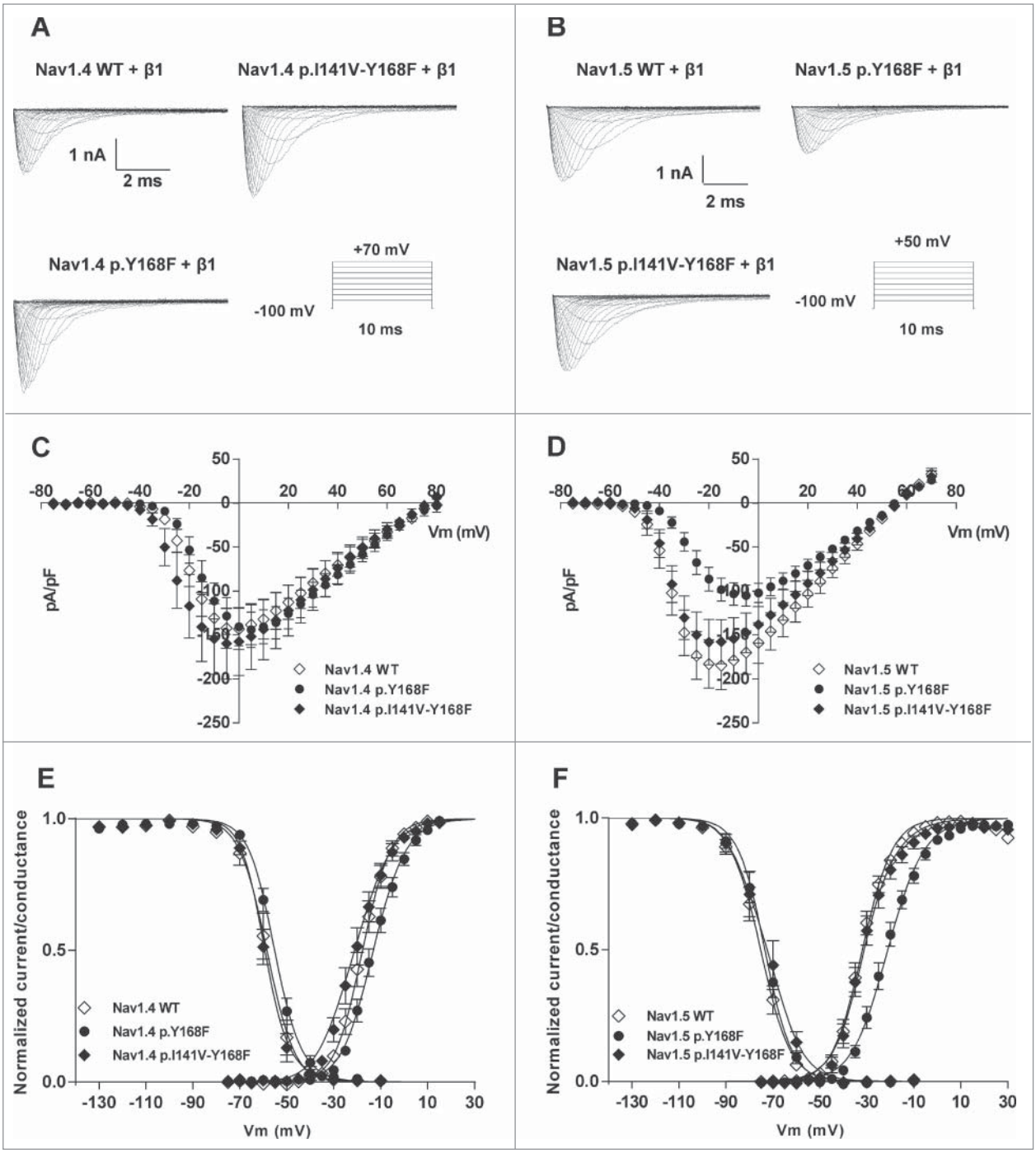

Figure 3. (**A and B**) Representative current traces obtained with the inset protocol from HEK293 cells transfected with WT and mutated $Na_v1.4$ channels (**A**); and WT and mutated $Na_v1.5$ channels (**B**). (**C and D**) Current-voltage relationship curves from WT and mutated $Na_v1.4$ channels (**C**); and WT and mutated $Na_v1.5$ channels (**D**). (**E and F**) Steady-state activation and inactivation curves for $Na_v1.4$ (**E**) and $Na_v1.5$ (**F**). Activation and inactivation properties were determined as described in **Figure 1**. Note that for the WT $Na_v1.4$ condition, I/V relationships, and the voltage dependences of activation and inactivation, the represented data in this figure are the same as in **Figure 1**.

in the p.I141V-Y168F mutant is due to the functional changes of both channels induced by the given mutation seems to be more probable.

On the other hand, the functional effects of the p.I141V, p.Y168F, and p.I141V-Y168F mutation were slightly different between Nav1.4 and Nav1.5 channels. For example, in the presence of the p.I141V mutation, a difference of 10 mV and 8 mV in the $V_{1/2}$ of steady-state activation was observed for Nav1.4, and Nav1.5, respectively. This difference may be due to different intrinsic protein interactions that stabilize the open confirmation

Table 1. Electrophysiological characteristics of Nav1.4 and Nav1.5 (p.I141V-Y168F, and p.Y168F)

	WT	p.I141V-Y168F	p.Y168F
Nav1.4 Activation	$V_{1/2} = -18 \pm 1.4$; $K = 5.3 \pm 0.4$; $n = 9$	$V_{1/2} = -20 \pm 1.8$; $K = 6.6 \pm 0.3$* ; $n = 7$	$V_{1/2} = -13 \pm 1.3$*; $K = 6.5 \pm 0.3$*; $n = 7$
Nav1.4 Inactivation	$V_{1/2} = -59 \pm 1.9$; $K = 5 \pm 0.2$; $n = 7$	$V_{1/2} = -59 \pm 1.6$; $K = 4.8 \pm 0.3$; $n = 8$	$V_{1/2} = -55 \pm 1.1$.; $K = 5.4 \pm 0.4$; $n = 8$
Nav1.5 Activation	$V_{1/2} = -32 \pm 1.3$; $K = 5.8 \pm 0.2$; $n = 11$	$V_{1/2} = -31 \pm 1.7$; $K = 6.3 \pm 0.5$; $n = 9$	$V_{1/2} = -21 \pm 1.4$***; $K = 7.2 \pm 0.3$**; $n = 11$
Nav1.5 Inactivation	$V_{1/2} = -75 \pm 1.6$; $K = 5.5 \pm 0.3$; $n = 11$	$V_{1/2} = -73 \pm 2.6$; $K = 6.1 \pm 0.4$; $n = 8$	$V_{1/2} = -73 \pm 1.6$; $K = 5.7 \pm 0.4$; $n = 9$

*$P < 0.05$.
**$P < 0.01$.
***$P < 0.001$.

in these 2 channels. Several studies demonstrated that the substitution of one VSD residue is sufficient to affect its function.[9,10] Although Nav1.4 and Nav1.5 are homologous channels with high sequence similarities, the environments of the S4 positive residues are not identical. This may result in different characteristics for the wild type channels and therefore may lead to different effects depending on the mutation that is introduced.

Altogether, these results highlight the functional role of 2 different segments (S1-S2) of the VSD in voltage-gated sodium channel gating, even though the exact interactions that influence the stability of the VSD are not yet fully understood.

Materials and Methods

Site-directed mutagenesis

Site-directed mutagenesis was performed on pRC-CMV-hSCN4A or pCDN3.1-hSCN5A using the Quick-Change II XL site-directed mutagenesis kit (Stratagene) according to the manufacturer's instructions.

Cell culture

Human Embryonic Kidney 293 cells (HEK293) were cultured at 37°C in Dulbecco's Modified Eagle Medium (DMEM) supplemented with 10% (Fetal bovine serum) FBS, 4 mM glutamine, and 20 mg/ml gentamicin in a humidified atmosphere of 5% CO2 and 95% air. All cell medium components, except glutamine (Sigma-Aldrich), were purchased from Gibco.

Cellular electrophysiology

The HEK293 cells were transfected with DNA complexed to JetPEI (Polyplus-transfection) according to the manufacturer's instructions. DNA concentrations were 1 μg of WT $Na_V1.4$ and $Na_V1.5$ channels: pRC-CMV-$Na_V1.4$ and pCDN3.1-$Na_V1.5$ for mutated channels; pRC-CMV-$Na_V1.4$-p.I141V, pRC-CMV-$Na_V1.4$.Y168F, or pRC-CMV-$Na_V1.4$-p.I141V-pY168F for $Na_V1.4$ and pCDN3.1- $Na_V1.5$-p.I141V, pCDN3.1-$Na_V1.5$-p.Y168F, or pCDN3.1- $Na_V1.5$-p.I141V-pY168F for $Na_V1.5$. In addition, 1 μg of pIRES-hβ1-CD8 was used as a gene reporter. Eight hours after transfection, the cells were isolated and seeded in plastic Petri dishes at low density. Twenty 4 hours after transfection, the resulting I_{Na} was recorded at room temperature (23–25°C), under whole-cell voltage clamp conditions with an Axopatch 200 B (Axon Instruments, Inc.) amplifier interfaced to a personal computer and driven by the PClamp 10 software (Molecular Devices Corporation). The cells were bathed with an extracellular solution containing (in mmol/L): NaCl 50, NMDG-Cl 80, CsCl 5, MgCl2 1.2, CaCl2 2, HEPES 10 and glucose 5. The pH was adjusted to 7.4 with CsOH. Glass pipettes (tip resistance: 1.2 to 3 MΩ) were filled with an intracellular medium containing (in mmol/L): CsCl 60, aspartic acid 50, CaCl2 1, MgCl2 1, HEPES 10, EGTA 11 and Na2ATP 5. pH was adjusted to 7.2 with CsOH.

Molecular modeling

The initial molecular model of $Na_v1.4$ was built using homology modeling and the crystal structure of the bacterial Na_vAb channel (PDB code 4EKW) served as a template.[7] Fifty different models of $Na_v1.4$ were built using MODELLER.[11] Ten were chosen based on their scoring functions (MOLDPF, DOPE and GA341). The quality of each model was analyzed using PROCHECK.[12] The structure with the highest number of residues in the core regions of the Ramachandran plot and the lowest number of residues in the disallowed regions was selected for the current study. The selected model contained 94% of residues in the core regions and no residues in the disallowed regions.

The selected structure of $Na_v1.4$ (both the native form and the I141V mutant) was embedded in a palmitoyl-oleyl-phosphatidylcholine (POPC) hydrated bilayer, surrounded by a KCl salt solution at a physiological concentration of 150 mM (total number of atoms: ~180, 000). The CHARMM22 with the CMAP correction and the CHARMM36 force fields were considered for the protein and the lipids, respectively.[13,14] Water was represented by the TIP3P model.[15]

The molecular dynamics simulations were performed using NAMD.[16] Langevin dynamics were applied to keep the temperature (300 K) and the pressure (1 atm) constant. The time-step of the simulations was 2.0 fs. Short- and long-range forces were calculated every 1 and 2 time-steps, respectively. Long-range electrostatics were calculated using Particle Mesh Ewald (PME). The cutoff distance of short-range electrostatics was taken to be 11 Å. A switching function was used between 8 and 11 Å to smoothly bring the vdW forces and energies to 0 at 11 Å. The equations of motion were integrated using a multiple time-step algorithm. During the calculations, chemical bonds between hydrogen and heavy atoms were constrained to their equilibrium values. Three d periodic boundary conditions were applied.

The following protocol of equilibration was used: 1) the entire protein was fixed for a 6 ns MD run in order to ensure the relaxation of

the lipids and the solution, 2) the backbone atoms were then constrained during an 8 ns MD run to enable subsequent reorganization of the side-chain groups, 3) the salt-bridges R225-E161, K228-E171, K228-D197, K175-E171 and K175-D197 in the DI VSD were also restrained, and 4) all constrains were released and the systems were further equilibrated for ~100 ns. The analysis of non-bonded energy was performed for the last 50 ns of the equilibration, for which the root mean square deviations (RMSD) from the initial structure of the channel calculated for the backbone atoms reached plateau.

Data analysis and statistical methods

The currents were analyzed with the Clampfit software (Axon Instruments, Inc.). The data were analyzed using a combination of pClamp10, Excel (Microsoft) and Prism (graphpad). The comparisons between groups were performed with 2-tailed Student's t test. All data shown are expressed as mean + SD. A P-value < 0.05 was considered significant.

Disclosure of Potential Conflicts of Interest

No potential conflicts of interest were disclosed.

Acknowledgments

We thank Dr. A. Felley for her useful comments on this manuscript. We acknowledge PRACE for awarding us access to resource CURIE based in FRANCE at the TGCC and SUPERMUC based in Germany at the LRZ. MK acknowledges MSU Supercomputer Lomonosov.

Funding

The group of HA was supported by a grant from the Swiss National Science Foundation (310030_147060).

References

1. Abriel H, Zaklyazminskaya EV. Cardiac channelopathies: genetic and molecular mechanisms. Gene 2013; 517:1-11; PMID:23266818; http://dx.doi.org/10.1016/j.gene.2012.12.061
2. Meisler MH, O'Brien JE, Sharkey LM. Sodium channel gene family: epilepsy mutations, gene interactions and modifier effects. J Physiol 2010; 588:1841-8; PMID:20351042; http://dx.doi.org/10.1113/jphysiol.2010.188482
3. Petitprez S, Tiab L, Chen L, Kappeler L, Rosler KM, Schorderet D, Abriel H, Burgunder JM. A novel dominant mutation of the Nav1.4 alpha-subunit domain I leading to sodium channel myotonia. Neurology 2008; 71:1669-75; PMID:19015483; http://dx.doi.org/10.1212/01.wnl.0000335168.86248.55
4. Swan H, Amarouch MY, Leinonen J, Marjamaa A, Kucera JP, Laitinen-Forsblom PJ, Lahtinen AM, Palotie A, Kontula K, Toivonen L, et al. A Gain-of-Function Mutation of the SCN5A Gene Causes Exercise-induced Polymorphic Ventricular Arrhythmias 2014; http://dx.doi.org/10.1161/CIRCGENETICS.114.000703
5. Cheng X, Dib-Hajj SD, Tyrrell L, Waxman SG. Mutation I136V alters electrophysiological properties of the Na(v)1.7 channel in a family with onset of erythromelalgia in the second decade. Mol Pain 2008; 4:1; PMID:18171466; http://dx.doi.org/10.1186/1744-8069-4-1
6. Lee MJ, Yu HS, Hsieh ST, Stephenson DA, Lu CJ, Yang CC. Characterization of a familial case with primary erythromelalgia from Taiwan. J Neurol 2007; 254:210-4; PMID:17294067; http://dx.doi.org/10.1007/s00415-006-0328-3
7. Payandeh J, Scheuer T, Zheng N, Catterall WA. The crystal structure of a voltage-gated sodium channel. Nature 2011; 475:353-8; PMID:21743477; http://dx.doi.org/10.1038/nature10238
8. Long SB, Tao X, Campbell EB, MacKinnon R. Atomic structure of a voltage-dependent K^+ channel in a lipid membrane-like environment. Nature 2007; 450:376-82; PMID:18004376; http://dx.doi.org/10.1038/nature06265
9. Lacroix JJ, Bezanilla F. Tuning the voltage-sensor motion with a single residue. Biophys J 2012; 103:L23-5; PMID:22947880; http://dx.doi.org/10.1016/j.bpj.2012.06.030
10. Lacroix JJ, Campos FV, Frezza L, Bezanilla F. Molecular bases for the asynchronous activation of sodium and potassium channels required for nerve impulse generation. Neuron 2013; 79:651-7; PMID:23972594; http://dx.doi.org/10.1016/j.neuron.2013.05.036
11. Eswar N, Webb B, Marti-Renom MA, Madhusudhan MS, Eramian D, Shen MY, Pieper U, Sali A. Comparative protein structure modeling using modeller. Curr Protoc Bioinforma 2006; Chapter 5:Unit 5 6; PMID:18429317; http://dx.doi.org/10.1002/0471140864.ps0209s50
12. Laskowski RA, MM. PROCHECK–a programm to check the stereochemical quality of protein structures. J Appl Cryst 1993; 26:283-91; http://dx.doi.org/10.1107/S0021889892009944
13. Mackerell AD, Feig M, Brooks CL. Extending the treatment of backbone energetics in protein force fields: limitations of gas-phase quantum mechanics in reproducing protein conformational distributions in molecular dynamics simulations. J Comput Chem 2004; 25:1400-15; PMID:15185334; http://dx.doi.org/10.1002/jcc.20065
14. Klauda JB, Venable RM, Freites JA, O'Connor JW, Tobias DJ, Mondragon-Ramirez C, Vorobyov I, MacKerell AD, Pastor RW. Update of the CHARMM all-atom additive force field for lipids: validation on six lipid types. J Phys Chem B 2010; 114:7830-43; PMID:20496934; http://dx.doi.org/10.1021/jp101759q
15. Jorgensen WL, Chandrasekhar J, Madura JD, Impey RW, Klein ML. Comparison of simple potential functions for simulating liquid water. J Chem Phys 1983; 79:926-35; http://dx.doi.org/10.1063/1.445869
16. Phillips JC, Braun R, Wang W, Gumbart J, Tajkhorshid E, Villa E, Chipot C, Skeel RD, Kalé L, Schulten K. Scalable molecular dynamics with NAMD. J Comput Chem 2005; 26:1781-802; PMID:16222654; http://dx.doi.org/10.1002/jcc.20289